J Mater Sci (2011) 46:700–706
DOI 10.1007/s10853-010-4797-5

Preparation of Sb_2S_3 film on functional organic self-assembled monolayers by chemical bath deposition

Gangqiang Zhu · Xijin Huang · Mirabbos Hojamberdiev · Peng Liu · Yun Liu · Guoqiang Tan · Jian-ping Zhou

Received: 14 April 2010 / Accepted: 26 July 2010 / Published online: 5 August 2010

Abstract In this work, self-assembled monolayers (SAMs) of octadecyltrichlorosilane (OTS) were applied to induce the nucleation and growth of the antimony sulfide (Sb_2S_3) films on the functional ITO glass substrate at low temperature. The structure, morphology, and optical properties of the Sb_2S_3 films were investigated by X-ray diffraction, scanning electron microscopy, X-ray energy dispersive spectroscopy, and UV–vis spectroscopy. After thermal treatment at 200 °C for 1 h in air, the orthorhombic Sb_2S_3 was formed as a predominant phase in the deposited thin films. When the deposited films were thermally treated at 400 °C for 1 h in air, the orthorhombic Sb_2S_3 was decomposed and a cubic Sb_2O_3 was formed. The optical band energies of the as-deposited and thermally treated Sb_2S_3 films at 200 °C for 1 h in air and nitrogen were found to be 2.05 eV, 1.77, and 1.76 eV, respectively. As chemical templates, the OTS-functionalized SAMs played an important role in controlling the nucleation and growth of Sb_2S_3 films at low temperature. The results obtained from different preparation parameters applied in the present work will allow controlling the growth of the Sb_2S_3 films with uniform surface.

G. Zhu (✉) · X. Huang · P. Liu · J. Zhou
School of Physics and Information Technology, Shaanxi Normal University, Xi'an 710062, People's Republic of China
e-mail: zgq2006@snnu.edu.cn

M. Hojamberdiev
Shaanxi Key Laboratory of Nano-Materials and Technology, Xi'an University of Architecture and Technology, Xi'an 710055, People's Republic of China

Y. Liu · G. Tan
School of Materials Science and Engineering, Shaanxi University of Science and Technology, Xi'an 710021, People's Republic of China

Introduction

Metal chalcogenide semiconductors have presented numerous potential applications, including biomedical labeling/imaging, light-emitting diodes (LEDs), lasers, and solar cells, because of their photostability, size-dependent broadband absorption, and narrow emission [1–6]. Antimony trisulfide (Sb_2S_3) is a member of the main-group metal chalcogenides, $A_2^{V}B_3^{VI}$ (where A = As, Sb, Bi and B = S, Se, Te) and has a high anisotropic orthorhombic layer structure [7]. Sb_2S_3 is a direct band gap semiconductor with excellent photoconductivity and high thermoelectric power [8]. Due to these characteristics, it can be widely used in television cameras, microwave devices, thermoelectric cooling, and other optoelectronic devices in the infrared region [9–12]. Most recently, the Sb_2S_3 thin films have gained a special attention owing to its band gap (1.72 eV), covering the visible and near infrared range of the solar spectrum. Because of good photosensitive and well-defined quantum effects, the Sb_2S_3 thin films have a potential application in solar energy conversion [13]. So far, a number of methods have been employed to prepare the Sb_2S_3 thin films, such as chemical bath deposition [14–17], spray pyrolysis [18], thermal vacuum evaporation [19, 20], and electro-deposition [21].

In recent years, there has been a growing interest in using two-dimensional organic layers with specific functional groups to initiate the nucleation of crystals to prepare solid thin films [22]. By simply mimicking the role of interfaces in nature, self-assembled monolayers (SAMs) on the different substrates are often employed to generate appropriate interfaces at which the synthesis of inorganic crystals can be realized. As structural and/or chemical templates, SAMs play an active role in controlling the nucleation and growth of inorganic crystals at near room temperature. The chemical bath deposition method is one of the low cost and

environment-friendly processes for solid thin film preparation. Until now, this technique has been mainly used to prepare thin oxide (ZrO_2, HfO_2, TiO_2, and SnO_2) films through a hydrolysis reaction [22–24]. To the best of our knowledge, a few works have been done on the preparation of the Sb_2S_3 films by SAMs-assisted chemical bath deposition technique. In this work, we therefore considered to fabricate the Sb_2S_3 films by chemical bath deposition method on the SAMs-functionalized ITO glass substrate at 35 °C for 12 h. The effects of thermal treatment temperature, deposition time, and the functional films on the morphologies and optical properties of the Sb_2S_3 films were investigated.

Experimental

Preparation and modification of SAMs

As a substrate, ITO glass samples were ultrasonically cleaned in acetone, ethanol, and deionized water. After drying at 50 °C for 30 min, the substrates were subjected to UV irradiation (184.9 nm) for 30 min using a low-pressure Hg lamp (PL16-110, Sen Lights Corp., Japan) in order to improve the hydrophilic property of the substrate. SAMs were prepared by immersing the cleaned and dried glass substrates into an anhydrous toluene (99.5%, water <0.03%) solution containing 1 vol% of octadecyltrichlorosilane (OTS) for 30 min. After drying in nitrogen atmosphere, the SAMs-deposited substrates were heated at 120 °C for 5 min to remove a residual solvent and promote chemisorption of the SAMs. After that, the samples were exposed to UV irradiation for 30 min, which modified the functional groups in the exposed areas and resulted in the change of the original hydrophobic groups.

Deposition of Sb_2S_3 films

Antimony sulfide (Sb_2S_3) films were deposited on the functional ITO glass substrates by self-assembled deposition at 35 °C. The starting materials employed were antimony trichloride ($SbCl_3 \cdot 2H_2O$) and sodium thiosulfate ($Na_2S_2O_3$). They were analytical grade and used without further purification. To prevent the hydrolysis of Sb^{3+} ions, 1.84 g $SbCl_3$ was initially dissolved in 5 mL HCl (1 mol/l) and then 3.0 g $Na_2S_2O_3$ was separately dissolved in 20 mL distilled water. After complete dissolution of the reactants, the $Na_2S_2O_3$ solution was poured drop-wise into the $SbCl_3$ solution under vigorous stirring, followed by the addition of 25 mL distilled water to make up the total volume 50 mL. The solution was homogenized by magnetic stirring for 5 min. The pH of the final solution was adjusted to 3 by the addition of ammonium hydroxide. Afterwards, the SAM-deposited substrates were immersed in the solution at 35 °C for 12 h in an incubator. The substrates were horizontally placed in the solution, and the SAMs-deposited side was upside down to prevent particles formed in the solution from accumulation on the substrate surface. After deposition, the substrates were taken out from the solution, rinsed repeatedly with distilled water, dried at 60 °C for 3 h, and thermally treated at 100, 200, 300, and 400 °C for 1 h in air. In order to analyze the effects of thermal treatment atmosphere on the optical properties of the Sb_2S_3 films, the SAMs-deposited substrate was thermally treated at 200 °C for 1 h in nitrogen.

Characterization

The crystalline structures of the films were determined by X-ray diffraction (XRD) using a D/MAX2550V diffractometer (Rigaku, Japan) with monochromated CuKα radiation ($\lambda = 1.5406$ Å) at 40 kV and 50 mA. The morphologies of the films were examined using a Quanta 200 scanning electron microscope (FEI, Netherlands) equipped with an X-ray energy dispersive spectroscopy (EDS). The UV–vis absorption spectra were measured using a Lambda 950 spectrophotometer (Perkin-Elmer, USA) in the wavelength range of 400–800 nm.

Results and discussion

Structure and morphology

Figure 1 shows the XRD patterns of the as-deposited and thermal treated Sb_2S_3 films at 100, 200, 300, and 400 °C

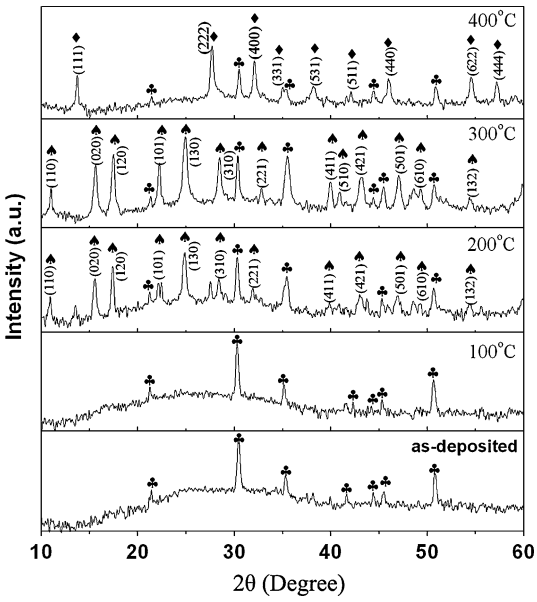

Fig. 1 XRD patterns of the as-deposited and thermal treated Sb_2S_3 films at 100 °C, 200 °C, 300 °C, and 400 °C for 1 h in air. *Key*: *club* ITO, *spade* Sb_2S_3, and *filled diamond* Sb_2O_3

for 1 h in air. The as-deposited and thermal treated samples at 100 °C do not show any characteristic peaks, excluding the peaks of the ITO glass substrate. After thermal treatment at 200 and 300 °C for 1 h, all the diffraction peaks in the XRD patterns are readily indexed to a pure orthorhombic phase of Sb_2S_3 (JCPDS card no. 42-1393). All the diffraction peaks in the XRD pattern of the sample thermally treated at 400 °C for 1 h correspond to a cubic phase of Sb_2O_3 (JCPDS card no. 75-1565) due to the decomposition of Sb_2S_3 and the formation of high crystalline cubic phase of Sb_2O_3.

The SEM micrographs of the as-deposited and thermal treated Sb_2S_3 films at 200, 300, and 400 °C for 1 h in air are represented in Figs. 2 and 3. Figure 2a shows a low-magnification SEM image of the as-deposited Sb_2S_3 films with a compact surface and well-composed nearly spherical particles. As shown in Fig. 2b, a detailed surface microstructure shows close-packed arrays of particles with a diameter of about 3 μm. The surface morphology without any distinctive changes and the particles with nearly spherical shapes in diameter of about 3 μm can also be observed after thermal treatment of the as-deposited film at 200 °C for 1 h (Fig. 2c, d). Figure 2e displays a lateral image of the cross-sectioned sample, confirming that the film composed of monolayer Sb_2S_3 particles with a hemispherical shape has a thickness of about 1.8 μm. According to the X-ray energy dispersive spectroscopy (EDS) results, the molar ratio of Sb:S obtained from the peak area (Fig. 2f) is 39:61, which is close to 2:3, giving a possible composition of Sb_2S_3. The effects of thermal treatment temperatures on the surface morphology of the as-deposited films are shown in Fig. 3. After thermal treatment at 300 °C for 1 h in air (Fig. 3a), the shape of the particles in the film was almost disappeared, and a porous monolith was formed. Figure 3b shows the morphology of the Sb_2O_3 film formed by thermal treatment at 400 °C for 1 h in air.

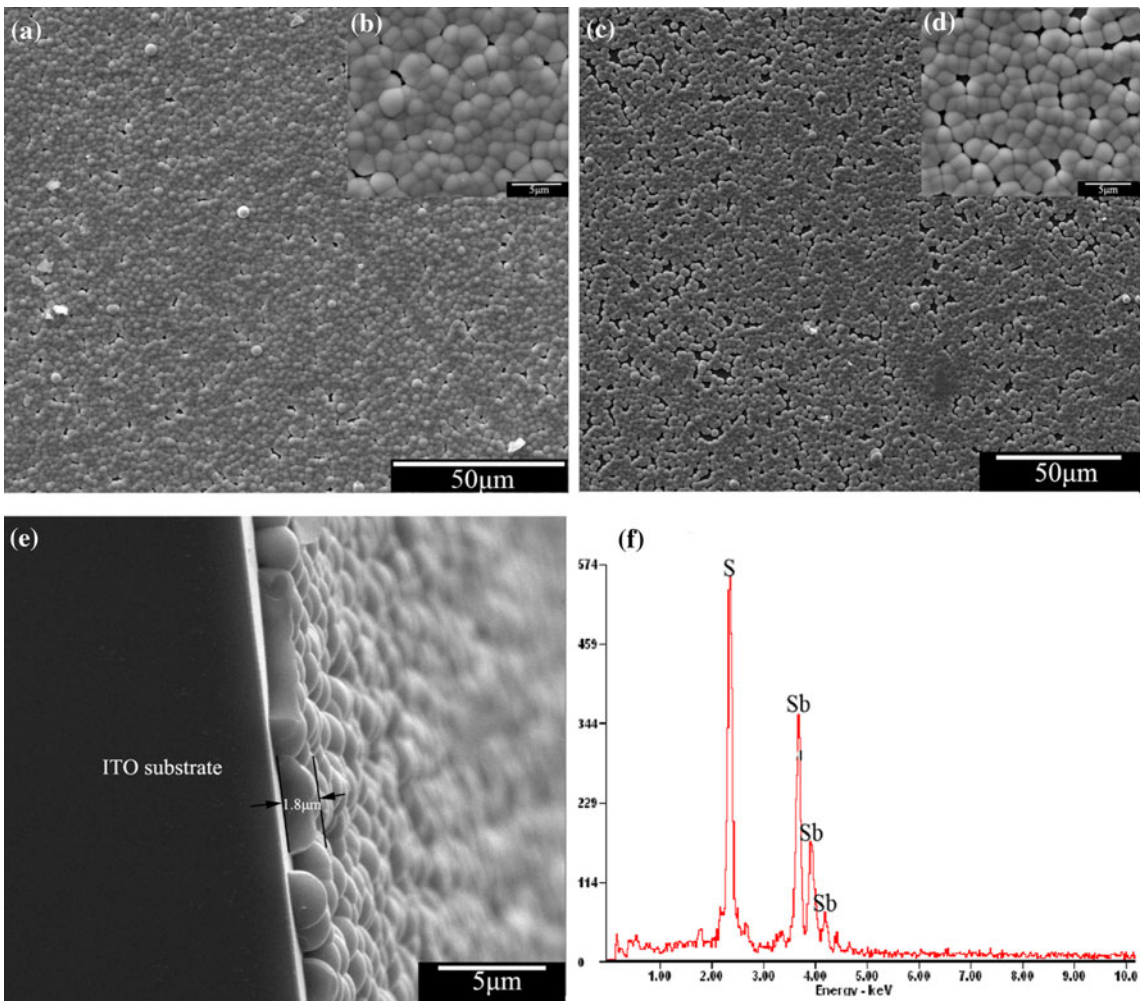

Fig. 2 SEM micrographs of the as-deposited (**a**, **b**) and thermal treated (**c**, **d**) Sb_2S_3 films at 200 °C for 1 h in air. A lateral SEM image (**e**) and EDS spectrum (**f**) of the Sb_2S_3 films thermally treated at 200 °C for 1 h in air

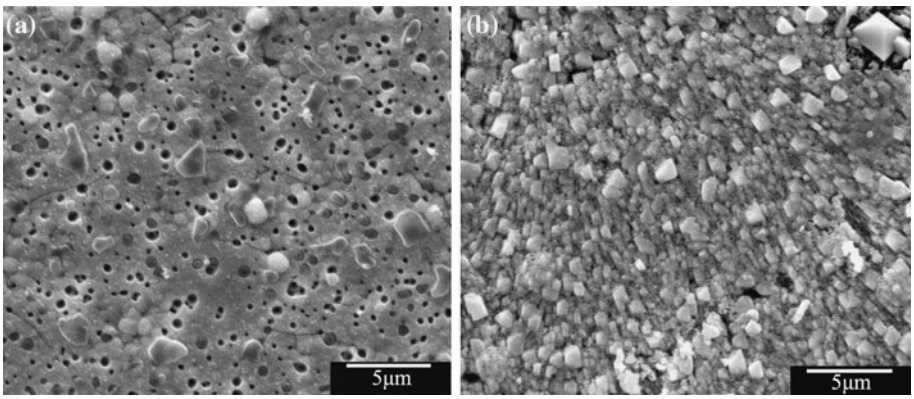

Fig. 3 SEM micrographs of the Sb_2S_3 films thermally treated at 300 °C (**a**) and 400 °C (**b**) for 1 h in air

Instead of nearly spherical particles of the Sb_2S_3 films, Sb_2O_3 crystallites with irregular shapes were formed on the ITO glass substrates (inset in Fig. 3b).

Effect of deposition time

In order to investigate the deposition process of the monolayer Sb_2S_3 films on the ITO glass substrate as a function of time, the substrates were immersed in the solution at 35 °C for different times (4, 6, 8, and 12 h). Figure 4 represents the SEM images of the Sb_2S_3 films as a function of deposition time. After immersing the ITO glass substrates in the solution for 4 h, some sphere-like particles in micrometer size were randomly distributed on the substrate surface (Fig. 4a). Apparently, the diameters of the spherical particles with smooth surface are 1.5–3 μm. With increasing the deposition time to 6 h, the number of deposited particles was increased in per unit area, resulting well compaction of particles, as shown in Fig. 4b. When the substrate was kept in the solution for 8 h (Fig. 4c), the particles compaction was further increased dramatically. Finally, a dense film with well-compacted particles was

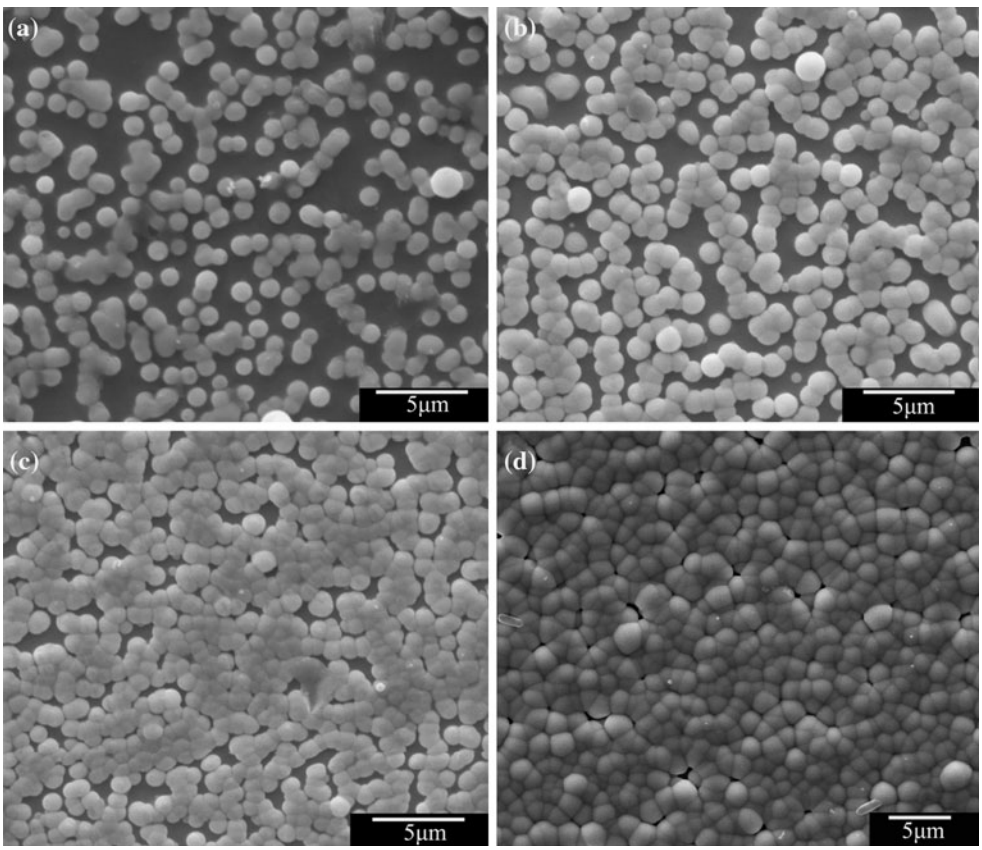

Fig. 4 SEM micrographs of the Sb_2S_3 films as a function of deposition time: 4 h (**a**), 6 h (**b**), 8 h (**c**), and 12 h (**d**)

obtained after the prolongation of the immersing time to 12 h (Fig. 4d).

Effect of the functional monolayer

Figure 5a shows the SEM image of the Sb_2S_3 film deposited on the nonfunctional ITO glass substrate. As can be seen, the shape of the particles is not clear, and only a few particles with spherical shapes were formed. In contrast, the film deposited on the functional ITO glass substrate had a monolayer of well-compacted particles with a nearly spherical shape (Fig. 2a). It can be concluded that the OTS functional SAMs induces the nucleation and growth of the Sb_2S_3 films. To investigate the role of OTS–SAMs, the contact angle of the as-deposited and UV-irradiated substrates was measured because it is a simple method for surface analysis related to surface energy and tension. Figure 5b shows the contact angle of diluted water drop on the as-deposited OTS film. The contact angle is about 108.8°, indicating the hydrophobic property of the film. When the ITO glass substrates were immersed in the OTS solution, the hydrolyzed organosilanes (OTS) were attached to the surface of the glass substrate by the formation of a covalent siloxane (Si–O–Si) bond, and they were condensed to each other, creating a SAM with a terminal CH_3 group to form Si–CH_3 group. So, diluted water could not spread out on the hydrophobic SAMs. After the SAMs were exposed to UV irradiation, diluted water could spread out on the substrate with contact angle about 10.2°, as shown in Fig. 5c, evidencing the hydrophilic characteristic of the film. After exposing to UV irradiation, the hydrophobic Si–CH_3 was destructed, and an extremely reactive Si radical was left on the surface, followed by immediate reaction with trace water to form polar functional silanol (Si–OH) groups. The functional Si–OH groups possessed a strong hydrophilic property and could adsorb precursors from the solution to form the Sb_2S_3 film uniform morphology.

Growth mechanism

The dissociation of thiosulphate mainly depends on the pH of the solution [15, 25]. In acidic solution, thiosulphate dissociates into S, but in alkaline solution it dissociates into S^{2+}.

$$S_2O_3^{2-} + H^+ \rightarrow S + HSO_3^- \quad (1)$$

$$S_2O_3^{2-} + 2H^+ \rightarrow S + SO_2 + H_2O \quad (2)$$

$$S_2O_3^{2-} + OH^- \rightarrow HS^- + SO_4^{2-} \quad (3)$$

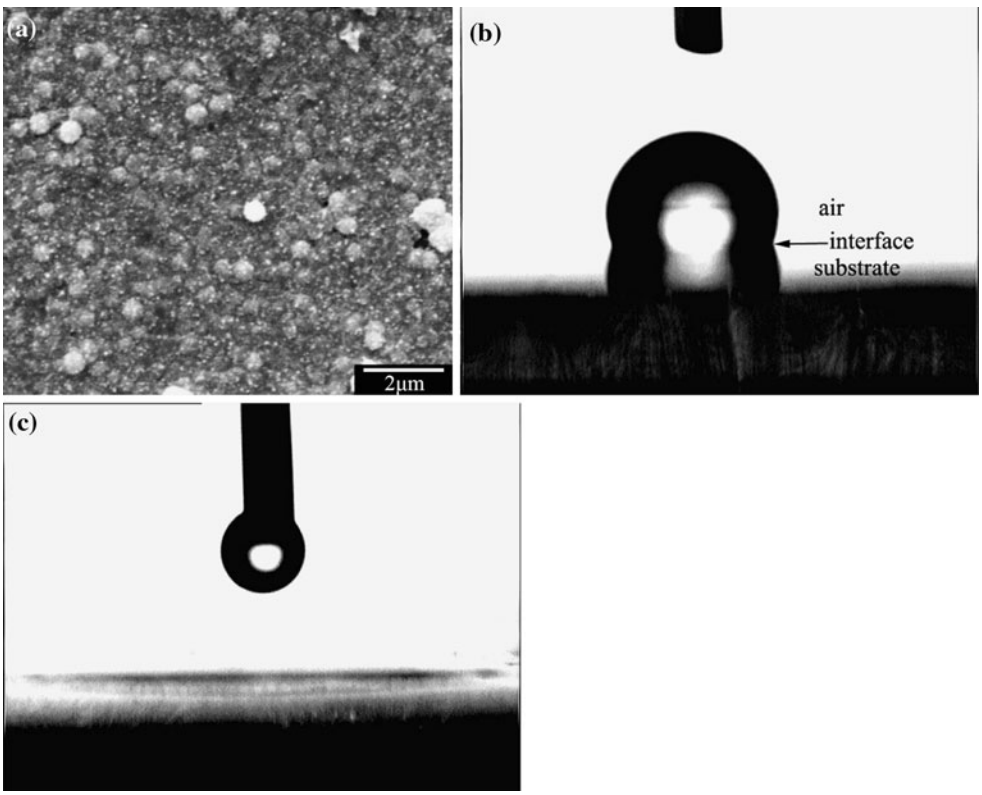

Fig. 5 SEM micrograph of the Sb_2S_3 film deposited on the nonfunctional ITO glass substrate (**a**). Micrographs of the contact angle on the OTS film-deposited substrate before (**b**) and after (**c**) exposing to UV irradiation

In this work, the deposition was performed in a relatively weak acidic solution at pH = 3. Hence, it might involve the formation reaction of S and its subsequent reduction to S^{2-}. It is well known that thiosulphate can form a very strong complex with metal ions, namely, Bi and Sb [14]. The metal–thiosulphate complexes undergo decomposition to form corresponding metal-sulfides. Therefore, we describe the formation mechanism of the uniform Sb_2S_3 films as follows: first, metal–thiosulphate complexes of $Sb_2(S_2O_3)_3$ were formed as a result of the reaction between $SbCl_3$ and $Na_2S_2O_3$, which was in turn hydrolyzed to form Sb_2S_3 precursors. At the same time, the Sb^{3+} and S^{2-} ions were produced through the decomposition of intermediate $Sb_2(S_2O_3)_3$, and a supersaturated solution was formed. The hydrophilic functional Si–OH groups on the substrates adsorbed the precursors of Sb_2S_3 from the solution. Moreover, the Sb_2S_3 precursors on the substrate further adsorbed the Sb^{3+} and S^{2-} ions from the supersaturated solution to grow up. Finally, with an increase in deposition time, the dense Sb_2S_3 films composed of well-compacted nearly spherical particles were formed.

$$2SbCl_3 + 3Na_2S_2O_3 \rightarrow Sb_2(S_2O_3)_3 + 6NaCl \quad (4)$$

$$Sb_2(S_2O_3)_3 + 6H_2O \rightarrow Sb_2S_3 + 3HSO_4^- + 3H_2O \quad (5)$$

$$Sb_2(S_2O_3)_3 \rightarrow 2Sb^{3+} + 3S_2O_3^{2-} \quad (6)$$

$$S_2O_3^{2-} + H_2O \leftrightarrow SO_4^{2-} + S^{2-} + 2H^+ \quad (7)$$

Optical properties

Figure 6 shows the UV–vis optical absorption spectra of the Sb_2S_3 films in the wavelength range of 400–800 nm. The curves of a, b, and c represent the absorption spectra for the as-deposited and thermal treated Sb_2S_3 films at 200 °C for 1 h in air and nitrogen, respectively. The optical data were analyzed at the near absorption edge using the equation: $\alpha = k(h\nu - E_g)^{n/2}/h\nu$, where k and n are

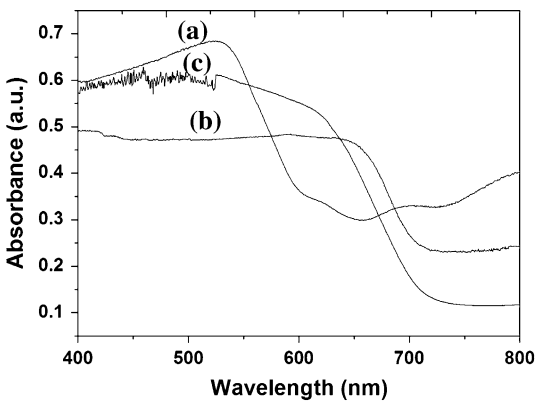

Fig. 6 UV–vis absorption spectra of the as-deposited (*a*) and thermal treated Sb_2S_3 films at 200 °C for 1 h in air (*b*) and nitrogen (*c*)

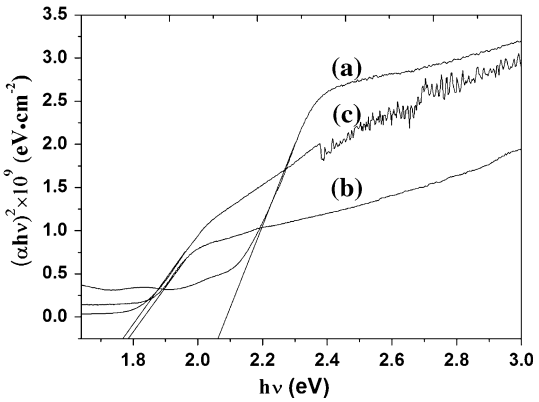

Fig. 7 Plot of $(\alpha h\nu)^2$ versus $h\nu$ of the as-deposited (*a*) and thermal treated Sb_2S_3 films at 200 °C for 1 h in air (*b*) and nitrogen (*c*)

constants and E_g is the band gap of the semiconductor. The value of n is equal to 1 for direct transition materials, including Sb_2S_3. As shown in Fig. 7, the plot of $(\alpha h\nu)^2$ versus $h\nu$ gives the E_g values at ca. 2.05, 1.77 and 1.76 eV, which shift to a higher energy in comparison with a typical direct band gap (1.70 eV) of bulk Sb_2S_3 crystal. These values are consistent with the previously reported values for the Sb_2S_3 films [15, 26].

Conclusions

Antimony sulfide (Sb_2S_3) films on the functional ITO glass substrate were prepared by chemical bath deposition method at low temperature. The ITO glass substrates were functionalized with the deposition of SAMs by using OTS. After thermal treatment at 200 °C for 1 h in air, the orthorhombic Sb_2S_3 was formed as a predominant phase in the deposited thin films. When the deposited films were thermally treated at 400 °C for 1 h in air, the orthorhombic Sb_2S_3 was decomposed and a cubic Sb_2O_3 was formed. The optical band energies of the as-deposited and thermally treated Sb_2S_3 films at 200 °C for 1 h in air and nitrogen were found to be 2.05 eV, 1.77, and 1.76 eV, respectively. As chemical templates, the OTS-functionalized SAMs played an important role in controlling the nucleation and growth of Sb_2S_3 films at low temperature.

References

1. Poudel B, Hao Q, Ma Y, Lan YC, Minnich A, Yu B, Yan X, Wang DZ, Muto A, Vashaee D, Chen XY, Liu JM, Dresselhaus MS, Chen G, Ren ZF (2008) Science 320:634
2. Disalvo FJ (1991) Science 247:649
3. Ennaoui A, Fiechter S, Pettenkofer Ch, Alonso-Vante N, Büker K, Bronold M, Höpfner C, Tributsch H (1993) Sol Energy Mater Sol Cells 29:289

4. Huynh WU, Dittmer JJ, Alivisatos AP (2002) Science 295:2425
5. Mitzi DB, Yuan M, Liu W, Kellock AJ, Chey SJ, Deline V, Schrott AG (2008) Adv Mater 20:3657
6. Vogel R, Hoyer P, Weller H (1994) J Phys Chem 98:3183
7. Srivastava SK, Pramanik M, Palit D, Haueseler H (2004) Chem Mater 16:4168
8. Desai JD, Lokhande CD (1995) J Non-Cryst Solids 181:70
9. Ghosh G, Varma BP (1979) Thin Solid Films 69:61
10. Grigas J, Meshkanskas J, Orlimas J (1976) Phys Status Solidi A 37:10
11. Chokalingam MJ, Rao KN, Rangarajan R, Suryanarayana CV (1970) J Phys D 3:629
12. Montrimass E, Pazera A (1976) Thin Solid Films 34:1641
13. Savadogo O, Mandal KC (1992) Sol Energy Mater Sol Cells 26:117
14. Messina S, Nair MTS, Nair PK (2007) Thin Solid Films 515:5777
15. Krishnan B, Arato A, Cardenas E, Das Roy TK, Castillo GA (2008) App Sur Sci 254:3200
16. Mane RS, Sankapal BR, Lokhande CD (1999) Thin Solid Films 353:29
17. Mane RS, Lokhande CD (2003) Mater Chem Phys 82:347
18. Killedar VV, Rajpure KY, Patil PS, Bhosale CH (1999) Mater Chem Phys 59:237
19. Ţigău N, Gheorghieş C, Rusu GI, Condurache-Bota S (2005) J Non-Cryst Solids 351:987
20. Montiimas E, Pazera A (1976) Thin Solid Films 34:65
21. Mandal KC, Mondal A (1990) J Phys Chem Solids 51:1339
22. Gao YF, Koumoto K (2005) Cryst Growth Des 5:1983
23. Gao YF, Masuda Y, Peng ZF, Yonezawa T, Koumoto K (2003) J Mater Chem 13:608
24. Shirahata N, Masuda Y, Yonezawa T, Koumoto K (2002) Langmuir 18:10379
25. Grozdanov I (1994) Semicond Sci Technol 9:1234
26. Nair MTS, Pena Y, Campos J, Garcia VM, Nair PK (1998) J Electrochem Soc 145:2113